

CIDER: A CAUSAL CURE FOR BRAND-OBSSESSED TEXT-TO-IMAGE MODELS

Fangjian Shen, Zifeng Liang, Chao Wang, Wushao Wen[†]

School of Computer Science and Engineering, Sun Yat-sen University, Guangzhou, China

ABSTRACT

Text-to-image (T2I) models exhibit a significant yet under-explored "brand bias", a tendency to generate contents featuring dominant commercial brands from generic prompts, posing ethical and legal risks. We propose CIDER, a novel, model-agnostic framework to mitigate bias at inference-time through prompt refinement to avoid costly retraining. CIDER uses a lightweight detector to identify branded content and a Vision-Language Model (VLM) to generate stylistically divergent alternatives. We introduce the Brand Neutrality Score (BNS) to quantify this issue and perform extensive experiments on leading T2I models. Results show CIDER significantly reduces both explicit and implicit biases while maintaining image quality and aesthetic appeal. Our work offers a practical solution for more original and equitable content, contributing to the development of trustworthy generative AI.

Index Terms— Generative AI, Text-to-Image Models, Brand Bias, Causal Inference, Prompt Engineering

1. INTRODUCTION

Recent breakthroughs in text-to-image (T2I) diffusion models [1, 2], such as Stable Diffusion [2] and many others [3, 4], have enabled the generation of high-fidelity and contextually relevant images. These models have found applications in wide-ranging domains, such as creative industries, design, and entertainment [4, 5]. However, most existing benchmarks focus heavily on text-image alignment and image quality [6, 7], overlooking other critical aspects such as the image's originality and the presence of biased content. Among these overlooked issues, brand bias stands out as a urgent challenge [8, 9].

Brand Bias is a tendency of T2I models that disproportionately generates contents featuring or alluding to specific, often globally dominant, commercial brands, even when the user's prompt is generic. This bias manifests in two distinct forms. The first is Explicit Brand Representation, which involves the direct rendering of registered logos or trademarks. The second, known as Implicit Brand Aesthetics, is a more insidious form. It refers to the replication of a brand's signature stylistic elements, which can include proprietary architectural designs, character archetypes, or unique product design philosophies. The unchecked proliferation of brand bias may carry significant negative consequences. Ethically and commercially, it can function as unintentional and free advertising, creating an uneven competition that favors established corporations. This could be further exploited through malicious data poisoning [10]. Legally, the unauthorized generation of trademarked logos and copyrighted designs presents a clear risk of infringement [11]. While previous works have been dedicated to mitigate biases in T2I models, their focus has predominantly been on societal biases [12, 13], leaving the pervasive issue of brand bias relatively unaddressed [8, 9]. Our research aims to fill this critical gap. We frame

[†]Corresponding author.



Fig. 1. Examples of brand bias in leading T2I models. For generic prompts, leading T2I models frequently generate images featuring specific commercial brands, demonstrating both explicit (logos) and implicit (aesthetics) forms of bias.

this problem through the lens of a Structural Causal Model (SCM) [14], a directed acyclic graph commonly used to describe the causal relationships within a system [15]. As depicted in Figure 2, the pre-trained knowledge D in T2I models confounds the system to generate biased images.

To address this challenge, we propose Causal Intervention for Debiasing Esthetic Representation (CIDER) framework, a novel and economic framework designed to mitigate brand bias through a model-agnostic prompt refinement strategy. Our approach first employs a lightweight detector to identify explicit and implicit brand bias in an image. Upon detecting a bias, CIDER initiates a semantic redirection process managed by a Vision-Language Model (VLM). Instead of simple negation, the VLM deconstructs the biased element into its core aesthetic features and generates a set of stylistically divergent yet semantically relevant concepts. These candidates are then ranked by a scoring function that maximizes the aesthetic distance from the biased brand while preserving thematic alignment with the prompt's core subject. Finally, the highest-scoring concepts are used to augment the original prompt. This refined prompt functions as a practical causal intervention, steering the generation process away from the biased observational distribution toward a

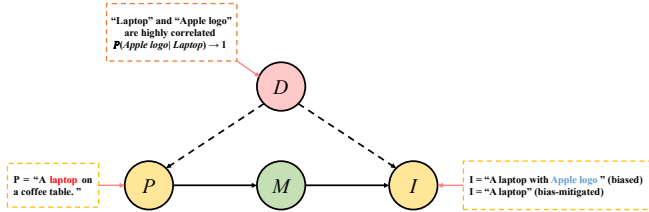


Fig. 2. Structural Causal Model for brand bias. Without causal intervention, the model produces an image with brand bias due to the spurious correlation between “laptop” and “Apple logo” caused by the confounding variable D . With our causal intervention, the constructed mediating variable M can block the backdoor paths for $P \rightarrow I$ opened by D and generate the bias-mitigated causal image.

bias-mitigation output. To improve efficiency, the mapping from a detected bias set to its optimal modifiers is cached for future requests. We summarize our findings and contributions as follows:

- We propose CIDER, an effective and economic framework that uses model-agnostic prompt to mitigate brand bias.
- We introduce the Brand Neutrality Score, a new benchmark designed to address the limitations of existing evaluations and provide a deeper understanding of brand bias in T2I models.
- We conduct extensive experiments on leading T2I models, showing that CIDER significantly reduces brand bias while maintaining high image quality.

2. THE CIDER FRAMEWORK

Brand bias in T2I models can be framed as a causal confounding problem. To eliminate this bias, a causal intervention is necessary. There are two primary methods, backdoor and front-door adjustment. The backdoor approach is intractable in this context. It would require directly observing and conditioning on the confounder D (the model’s training data), which is unobservable as it is implicitly encoded in the model’s weights and, hence, intractable in this context. Thus, our goal is to identify the causal relations between the prompt P and the image I from T2I models. D builds a backdoor path between P and I and misguides the T2I models to attend to brand-related contents to generate the biased image. To mitigate this spurious correlation, we block the backdoor path with front-door adjustment by introducing a mediator M , as shown in Figure 2.

The CIDER framework is designed as a practical, multi-stage implementation of this front-door intervention without any costly retraining or fine-tuning. As illustrated in Figure 3, CIDER consists of three main stages: (1) a lightweight Bias Detector, (2) an LLM-driven Prompt Refinement module that generates the mediator M , and (3) an efficiency-focused Redirection Cache.

2.1. Initial Generation and Bias Detection

Given an original prompt P , the T2I model first generates an initial image $I = \mathcal{T}(P)$, which is governed by the conditional probability $p(I|P)$. This image I then serves as input for our bias detector. The detector comprises two complementary sub-modules, EBRD and IBAD, to identify both explicit and implicit biases.

Explicit Brand Representation Detector (EBRD): This module identifies registered logos or trademarks. We employ a standard object detection model [16] fine-tuned on the LogoDet-3K dataset [17].

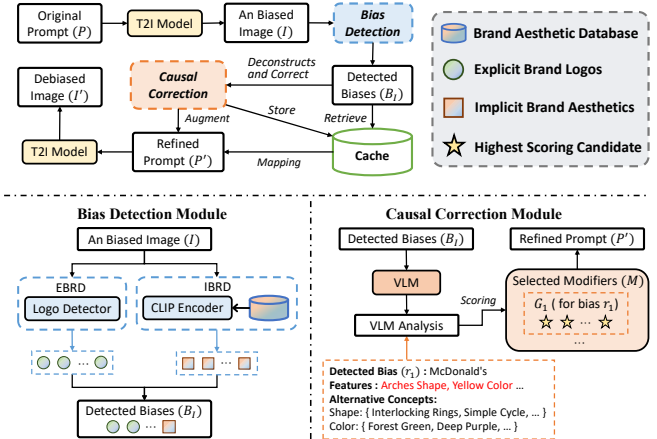


Fig. 3. The Overview of CIDER. The top panel presents a high-level overview of our inference-time intervention pipeline, highlighting the two core stages. The bottom panels provide detailed schematics for the Bias Detection Module and the Causal Correction Module. The legend in the top right explains the visual language used.

For a given image I , the EBRD module identifies and outputs a set of high-confidence explicit brand representations, denoted as L_I .

Implicit Brand Aesthetics Detector (IBAD): This module identifies stylistic similarities to known brand aesthetics. We first construct a Brand Aesthetics Database, a curated collection of images representing the signature styles of various brands (e.g., “Disney’s architectural style”). For each style, we pre-compute and store the CLIP [18] image embedding. For a given image I , we compute its CLIP embedding and measure its cosine similarity to each embedding in our database. Any brand aesthetic with a sufficiently high similarity score is considered a match. The set of these detected matches forms the output of implicit biases, C_I . The union $B_I = L_I \cup C_I$ forms the complete set of detected brand biases for image I .

2.2. Prompt Refinement by Causal Intervention

Upon detecting a non-empty bias set B_I , CIDER initiates its core refinement process. This stage generates our mediator variable M —a set of debiasing modifiers. To minimize latency and computational cost from repeated VLM calls, we first consult our Redirection Cache, which maps previously seen bias sets to optimal modifiers. If a cached entry covers the detected biases in B_I , the corresponding modifiers are retrieved directly. If no suitable cache entry exists, the image I and its detected bias set B_I are passed to a powerful VLM \mathcal{M}_s . For each identified bias $r_i \in B_I$, \mathcal{M}_s deconstructs it into a set of core aesthetic and semantic features, F_{r_i} . Then, \mathcal{M}_s proposes a set of alternative concepts, A_j , designed to be stylistically divergent yet within the same semantic category for each feature in F_{r_i} . To select the optimal alternative, we score each candidate modifier $a_k \in A_j$, using a function that balances aesthetic divergence from the bias with semantic relevance to the prompt’s core subject. The score S for a candidate a_k is:

$$S(a_k) = w \cdot (1 - \cos(E_{a_k}, E_f)) + (1 - w) \cdot \cos(E_{a_k}, E_p) \quad (1)$$

where E_{a_k} , E_f , E_p are the CLIP text embeddings for the candidate modifier, the feature, and the prompt’s core subject, respectively, and w is the weighting hyperparameter. We then select the

highest-scoring candidates to form set G_i for each bias r_i . The union of all sets G_i forms the final mediator M . This selection process defines the probability $p(M|I, P)$. The original prompt P is augmented with the selected modifiers M to create a refined prompt P' . The final debiased image $I' = \mathcal{T}(P')$ is generated based on this new prompt, a step captured by the probability $p(I'|M, P)$. The entire process realizes the front-door adjustment formula:

$$p(I'|do(P)) = \sum_{i,m} p(I'|M, P) \cdot p(M|I, P) \cdot p(I|P) \quad (2)$$

Finally, the mapping from the bias set B_I to the newly generated modifiers M is stored in the Cache to accelerate future interventions.

2.3. Brand Neutrality Score

Existing metrics for brand bias are often insufficient as they rely on a simple counts, ignoring that the visual salience of a single prominent brand element can be more impactful than several peripheral ones. We therefore introduce the Brand-Neutrality Score (BNS), a novel metric that provides a more nuanced, weighted measure of brand bias. For a given image I , we first use \mathcal{M}_s to identify all present brand biases and their confidence scores. These scores are sorted in descending order (s_1, s_2, \dots, s_n) . The BNS is calculated as:

$$\text{BNS}(I) = \exp(-\alpha \cdot \Phi_B(I)), \text{ where } \Phi_B(I) = \sum \gamma^{i-1} s_i \quad (3)$$

The penalty term $\Phi_B(I)$ is governed by two hyperparameters. The decay factor γ ensures that the most prominent bias contributes the most to the penalty, with subsequent biases having progressively less impact. The scaling factor α controls the sensitivity of the final score to the total penalty, tuning the steepness of the penalty curve analogous to an inverse temperature. For all experiments, we set the hyperparameters to $\gamma = 0.9$ and $\alpha = 0.75$. The value for γ was chosen to prevent the penalty from diminishing too rapidly when an image contains multiple biased elements. The value for α ensures the final scores fall within a well-distributed and interpretable range, maintaining a clear distinction between different degrees of bias.

3. EXPERIMENTAL SETUP

Model Choices We evaluated our framework on four state-of-the-art T2I models: the closed-source **Imagen 4** [19], **Seedream 3.0** [20], the open-source **Stable Diffusion XL** [21], and **FLUX.1** [22]. Notably, we intentionally excluded **DALL-E** [23] from our experiments because preliminary assessments revealed that its aggressive internal safety filters and post-processing routines often preemptively remove branded content, making it an uninformative testbed for our study. The chosen models, in contrast, provide a more suitable environment for analyzing the nuanced effects of brand bias and validating the efficacy of our mitigation framework.

Dataset To systematically probe brand bias, we constructed Brand-Bench, a curated benchmark of 220 custom prompts. The dataset is structured into two parts: the first one contains 100 single-bias prompts across ten diverse domains (e.g., technology, food, apparel) for analyzing domain-specific biases. The second part consists of 120 complex, combinatorial prompts designed to test our framework’s robustness by evoking multiple, interacting biases.

Configurations All experiments were conducted with standardized configurations to ensure consistency and reproducibility. The core of our CIDER framework is driven by a carefully engineered prompt



Fig. 4. Qualitative comparison of CIDER against baseline methods. Our method, CIDER, effectively removes the target brand bias while generating high-quality, stylistically coherent alternatives.

designed to guide the VLM. For the VLM, we utilize Gemini 2.5 Pro. To ensure high-quality, programmatically parsable outputs for our automated pipeline, this prompt instructs the VLM to adopt the persona of a visual culture and semiotics expert. It then directs the model to execute the precise three-step task described in 2.2 (Identify biases, Deconstruct features, Generate alternatives), supported by few-shot examples.

Evaluation Metrics To evaluate the bias mitigation and image quality. We used several metrics: our proposed BNS described in Section 2.3, Aesthetics [24], PickScore [25], and HPSv2 [26]. Aesthetics predicts human-perceived visual quality, typically using a linear probe on CLIP embeddings. PickScore measures the alignment between an image and a text prompt based on learned human preferences. Similarly, HPSv2 is a trained scoring function that reflects general human preferences over generated images. All metrics are reported with higher values indicating better performance.

4. EXPERIMENTAL RESULTS

4.1. Main Results

We evaluated each of the four T2I models under three distinct conditions: (a) Baseline, using the original prompts; (b) Negative Prompting, a common heuristic where keywords like “no logo” are appended; and (c) CIDER, our full proposed framework.

As illustrated in Table 1. The baseline generations confirm

Table 1. Main quantitative results and ablation study, showing percentage changes relative to the baseline. **Green** indicate an improvement over the baseline, while **Red** indicate a decline.

Model	Method	BNS(%)	Aesthetics	PickScore	HPSv2(%)
Imagen 4	Baseline	29.70	6.30	22.95	29.28
	Negative Prompting	38.75(+30.5%)	6.03(-4.2%)	22.66(-1.3%)	28.61(-2.3%)
	CIDER (w/o Scoring)	41.65(+40.2%)	6.16(-2.2%)	22.39(-2.4%)	28.29(-3.4%)
	CIDER (Full)	43.89 (+47.8%)	6.26(-0.7%)	22.43(-2.3%)	28.47(-2.8%)
SDXL	Baseline	32.38	6.39	22.81	29.79
	Negative Prompting	38.84(+19.9%)	6.12(-4.3%)	21.39(-6.2%)	29.08(-2.4%)
	CIDER (w/o Scoring)	37.97(+17.3%)	6.23(-2.7%)	22.21(-2.6%)	29.03(-2.5%)
	CIDER (Full)	51.78 (+59.9%)	6.24(-2.6%)	22.38(-1.9%)	29.30(-1.6%)
FLUX.1	Baseline	31.83	6.37	22.35	28.50
	Negative Prompting	33.73(+6.0%)	6.18(-2.9%)	22.21(-0.7%)	28.09(-1.4%)
	CIDER (w/o Scoring)	35.75(+12.3%)	6.14(-3.7%)	22.03(-1.4%)	27.96(-1.9%)
	CIDER (Full)	46.48 (+46.0%)	6.22(-2.4%)	22.07(-1.3%)	28.11(-1.4%)
Seedream	Baseline	29.94	6.30	22.90	29.08
	Negative Prompting	38.84(+29.7%)	6.28(-0.3%)	22.87(-0.1%)	28.58(-1.7%)
	CIDER (w/o Scoring)	34.71(+15.9%)	6.19(-1.7%)	22.40(-2.2%)	28.35(-2.5%)
	CIDER (Full)	48.91 (+63.4%)	6.27(-0.4%)	22.48(-1.9%)	28.49(-2.0%)

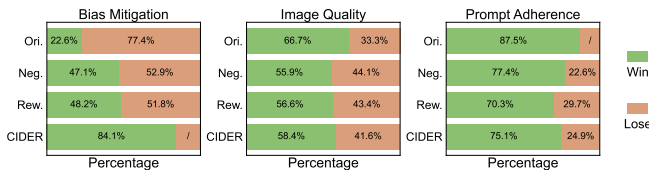


Fig. 5. Human evaluation results.

that all tested models exhibit significant brand bias. The Negative Prompting strategy yields only a marginal improvement in BNS. Furthermore, it frequently fails to completely remove biases and this minor improvement comes at a direct cost to image quality. In sharp contrast, CIDER achieves the best performance across the board. This demonstrates that CIDER successfully resolves the critical trade-off between bias removal and image fidelity, achieving both objectives simultaneously.

4.2. Ablation Study

We conducted comprehensive ablation studies to validate the contribution of each key component within the CIDER.

Scored Candidate Selection. To validate our multi-candidate selection process, we compared the full CIDER framework against a "direct-rewrite" baseline (CIDER w/o Scoring). The results in Table 1 show that our full framework significantly outperforms the direct-rewrite approach in bias mitigation, improving the average Brand Neutrality Score (BNS) by 28.2% across all models. Notably, this substantial gain in debiasing is achieved while maintaining a comparable, and in some cases slightly improved, level of aesthetic quality. This finding demonstrates that our scored selection process is the critical component for achieving the most effective degree of bias removal without penalizing image fidelity.

Hyperparameter Analysis. Figure 6 shows our hyperparameter study for the scoring weight w , which balances aesthetic divergence and semantic relevance on Seedream. We found lower values tend to substitute one brand bias for another, while higher values produce incoherent concepts that cause the T2I model to revert to its strong learned priors. The best performance was observed with $w = 0.4$, which served as the the default setting for all main experiments.

Redirection Cache. To evaluate the efficiency gains from the Redirection Cache, we measured the cumulative number of VLM calls

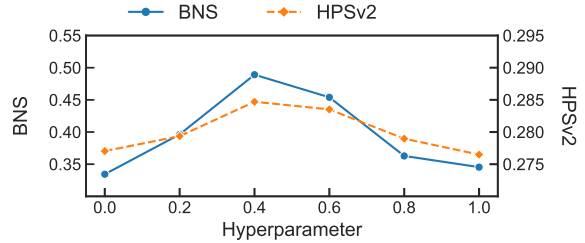


Fig. 6. Hyperparameter sensitivity analysis for w .

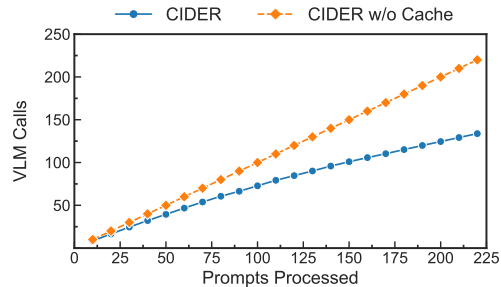


Fig. 7. Ablation Study of CIDER on redirection cache.

required to process our dataset. To ensure robust results, we report the average over 20 independent runs with randomly shuffled data. As illustrated in Figure 7, with the cache, the VLM calls volume flattens dramatically after an initial warm-up phase instead of scaling linearly. This finding demonstrates that the cache significantly reduces computational overhead, affirming its role in making CIDER both effective and economical.

4.3. Human Evaluation.

We conducted a human evaluation study using graduate students from top-tier universities as expert evaluators. For a selected subset of prompts, we presented images generated by each method in a randomized and anonymous order. Evaluators were instructed to select any image(s) they deemed superior based on three criteria: (1) Bias Mitigation, (2) Image Quality, and (3) Prompt Adherence. A "win" was recorded for a method each time one of its generated images was selected. We then calculated the overall win rate for each method by aggregating these selections across all evaluators and prompts. Figure 5 demonstrates the success of our method, providing strong substantiation for our central claims.

5. CONCLUSION

In this work, we present a systematic solution to brand bias, a critical yet under-explored issue in text-to-image models. We begin by formalizing brand bias within a causal framework and introduce CIDER, a novel, model-agnostic framework that performs an inference-time causal intervention by intelligently refining prompts. Our experiments first confirm the pervasiveness of this bias across leading T2I models and then demonstrate that CIDER effectively eliminates both explicit and implicit biases without compromising image quality. Our work enhances the understanding of commercial biases in generative AI and contributes to the development of fairer, more legally compliant, and trustworthy systems.

6. REFERENCES

- [1] Jonathan Ho, Ajay Jain, and Pieter Abbeel, “Denoising diffusion probabilistic models,” *Advances in neural information processing systems*, vol. 33, pp. 6840–6851, 2020.
- [2] Robin Rombach, Andreas Blattmann, Dominik Lorenz, Patrick Esser, and Björn Ommer, “High-resolution image synthesis with latent diffusion models,” in *Proceedings of the IEEE/CVF conference on computer vision and pattern recognition*, 2022, pp. 10684–10695.
- [3] Florinel-Alin Croitoru, Vlad Hondru, Radu Tudor Ionescu, and Mubarak Shah, “Diffusion models in vision: A survey,” *IEEE transactions on pattern analysis and machine intelligence*, vol. 45, no. 9, pp. 10850–10869, 2023.
- [4] Ling Yang, Zhilong Zhang, Yang Song, Shenda Hong, Runsheng Xu, Yue Zhao, Wentao Zhang, Bin Cui, and Ming-Hsuan Yang, “Diffusion models: A comprehensive survey of methods and applications,” *ACM computing surveys*, vol. 56, no. 4, pp. 1–39, 2023.
- [5] Hyung-Kwon Ko, Gwanmo Park, Hyeon Jeon, Jaemin Jo, Juho Kim, and Jinwook Seo, “Large-scale text-to-image generation models for visual artists’ creative works,” in *Proceedings of the 28th international conference on intelligent user interfaces*, 2023, pp. 919–933.
- [6] Tsung-Yi Lin, Michael Maire, Serge Belongie, James Hays, Pietro Perona, Deva Ramanan, Piotr Dollár, and C Lawrence Zitnick, “Microsoft coco: Common objects in context,” in *European conference on computer vision*. Springer, 2014, pp. 740–755.
- [7] Scott Reed, Zeynep Akata, Honglak Lee, and Bernt Schiele, “Learning deep representations of fine-grained visual descriptions,” in *Proceedings of the IEEE conference on computer vision and pattern recognition*, 2016, pp. 49–58.
- [8] Naveed Akhtar Jordan Vice, Richard Hartley, and Ajmal Mian, “Quantifying bias in text-to-image generative models,” *arXiv preprint arXiv:2312.13053*, vol. 2, 2023.
- [9] Mahammed Kamruzzaman, Hieu Minh Nguyen, and Gene Louis Kim, ““Global is Good, Local is Bad?” semicolon understanding brand bias in llms,” *arXiv preprint arXiv:2406.13997*, 2024.
- [10] Esben Kran, Hieu Minh Nguyen, Akash Kundu, Sami Jawhar, Jinsuk Park, Mateusz Maria Jurewicz, et al., “Darkbench: Benchmarking dark patterns in large language models,” *arXiv preprint arXiv:2503.10728*, 2025.
- [11] Zhenhua Xu, Xubin Yue, Zhebo Wang, Qichen Liu, Xixiang Zhao, Jingxuan Zhang, Wenjun Zeng, Wengpeng Xing, Dezhong Kong, Changting Lin, et al., “Copyright protection for large language models: A survey of methods, challenges, and trends,” *arXiv preprint arXiv:2508.11548*, 2025.
- [12] Isabel O Gallegos, Ryan A Rossi, Joe Barrow, Md Mehrab Tanjim, Sungchul Kim, Franck Dernoncourt, Tong Yu, Ruiyi Zhang, and Nesreen K Ahmed, “Bias and fairness in large language models: A survey,” *Computational Linguistics*, vol. 50, no. 3, pp. 1097–1179, 2024.
- [13] Yufei Guo, Muzhe Guo, Juntao Su, Zhou Yang, Mengqiu Zhu, Hongfei Li, Mengyang Qiu, and Shuo Shuo Liu, “Bias in large language models: Origin, evaluation, and mitigation,” *arXiv preprint arXiv:2411.10915*, 2024.
- [14] Jonas Peters, Dominik Janzing, and Bernhard Schölkopf, *Elements of causal inference: foundations and learning algorithms*, The MIT press, 2017.
- [15] Judea Pearl, *Causality*, Cambridge university press, 2009.
- [16] Rejin Varghese and M Sambath, “Yolov8: A novel object detection algorithm with enhanced performance and robustness,” in *2024 International conference on advances in data engineering and intelligent computing systems (ADICS)*. IEEE, 2024, pp. 1–6.
- [17] Jing Wang, Weiqing Min, Sujuan Hou, Shengnan Ma, Yuanjie Zheng, and Shuqiang Jiang, “Logodet-3k: A large-scale image dataset for logo detection,” *ACM Transactions on Multimedia Computing, Communications, and Applications (TOMM)*, vol. 18, no. 1, pp. 1–19, 2022.
- [18] Alec Radford, Jong Wook Kim, Chris Hallacy, Aditya Ramesh, Gabriel Goh, Sandhini Agarwal, Girish Sastry, Amanda Askell, Pamela Mishkin, Jack Clark, et al., “Learning transferable visual models from natural language supervision,” in *International conference on machine learning*. Pmlr, 2021, pp. 8748–8763.
- [19] Chitwan Saharia, William Chan, Saurabh Saxena, Lala Li, Jay Whang, Emily L Denton, Kamyar Ghasemipour, Raphael Gontijo Lopes, Burcu Karagol Ayan, Tim Salimans, et al., “Photorealistic text-to-image diffusion models with deep language understanding,” *Advances in neural information processing systems*, vol. 35, pp. 36479–36494, 2022.
- [20] Yu Gao, Lixue Gong, Qiushan Guo, Xiaoxia Hou, Zhichao Lai, Fanshi Li, Liang Li, Xiaochen Lian, Chao Liao, Liyang Liu, et al., “Seedream 3.0 technical report,” *arXiv preprint arXiv:2504.11346*, 2025.
- [21] Dustin Podell, Zion English, Kyle Lacey, Andreas Blattmann, Tim Dockhorn, Jonas Müller, Joe Penna, and Robin Rombach, “Sdxl: Improving latent diffusion models for high-resolution image synthesis,” *arXiv preprint arXiv:2307.01952*, 2023.
- [22] Stephen Batifol, Andreas Blattmann, Frederic Boesel, Saksham Consul, Cyril Diagne, Tim Dockhorn, Jack English, Zion English, Patrick Esser, Sumith Kulal, et al., “Flux. 1 kontext: Flow matching for in-context image generation and editing in latent space,” *arXiv e-prints*, pp. arXiv–2506, 2025.
- [23] Aditya Ramesh, Mikhail Pavlov, Gabriel Goh, Scott Gray, Chelsea Voss, Alec Radford, Mark Chen, and Ilya Sutskever, “Zero-shot text-to-image generation,” in *International conference on machine learning*. Pmlr, 2021, pp. 8821–8831.
- [24] Gabriel Ilharco, Mitchell Wortsman, Ross Wightman, Cade Gordon, Nicholas Carlini, Rohan Taori, Achal Dave, Vaishaal Shankar, Hongseok Namkoong, John Miller, Hannaneh Hajishirzi, Ali Farhadi, and Ludwig Schmidt, “Openclip,” July 2021.
- [25] Yuval Kirstain, Adam Polyak, Uriel Singer, Shahbuland Matiana, Joe Penna, and Omer Levy, “Pick-a-pic: An open dataset of user preferences for text-to-image generation,” *Advances in neural information processing systems*, vol. 36, pp. 36652–36663, 2023.
- [26] Xiaoshi Wu, Yiming Hao, Keqiang Sun, Yixiong Chen, Feng Zhu, Rui Zhao, and Hongsheng Li, “Human preference score v2: A solid benchmark for evaluating human preferences of text-to-image synthesis,” *arXiv preprint arXiv:2306.09341*, 2023.